Contribution of dust and elemental carbon to the reduction of snow albedo in the Indian Himalaya and the Finnish Arctic

Jonas Svensson[1], Johan Ström[2], Niku Kivekäs[1], Nathaniel B. Dkhar[3,4], Shresth Tayal[3,4], Ved P. Sharma[3,4], Arttu Jutila[5], John Backman[1], Aki Virkkula[1], Meri Ruppel[6], Antti Hyvärinen[7], Anna Kontu[8], Henna-Reetta Hannula[8], Matti Leppäranta[5], Rakesh K. Hooda[1,3], Atte Korhola[6], Eija Asmi[1], Heikki Lihavainen[1]

[1]Atmospheric Composition Research, Finnish Meteorological Institute, Helsinki, Finland
[2]Department of Environmental Science and Analytical Chemistry, Stockholm University, Stockholm, Sweden
[3]The Energy and Resource Institute, New Delhi, India
[4]The Energy and Resource Institute University, New Delhi, India
[5]Department of Physics, University of Helsinki, Helsinki, Finland
[6]Department of Environmental Sciences, University of Helsinki, Helsinki, Finland
[7]Expert Services, Finnish Meteorological Institute, Helsinki, Finland
[8]Arctic Research Center, Finnish Meteorological Institute, Sodankylä, Finland

Correspondence to J. Svensson (jonas.svensson@fmi.fi)

1 Abstract

Light-absorbing impurities (LAI) have the potential to substantially affect snow albedo, with subsequent changes on snow melt and impact on climate. To more accurately quantify the snow albedo, the contribution from different LAI needs to be assessed. Here we estimate the main LAI components, elemental carbon (EC) (as a proxy for black carbon) and mineral dust in snow from Indian Himalaya and compared it to snow samples from Arctic Finland. The impurities are collected onto quartz filters and are analyzed thermal-optically for EC, as well as with an additional optical measurement to estimate the light-absorption of dust separately on the filters. Laboratory tests were conducted using substrates containing soot and mineral particles specially prepared to test the experimental setup. Analyzed ambient snow samples show EC concentrations that are in the same range as presented by previous research, for each respective region. In terms of the mass absorption cross section (MAC) our ambient EC had surprisingly about half of the MAC value compared to our laboratory standard EC (chimney soot), suggesting a less light absorptive EC in the snow, which has consequences for the snow albedo reduction caused by EC. In the Himalayan samples, larger contributions by dust (in the range of 50 % or greater for the light absorption caused by the LAI) highlighted the importance of dust acting as a light absorber in the snow. Moreover, EC concentrations in the Indian samples, acquired from a 120 cm deep snow pit (covering possibly the last five years of snow fall), suggest an increase in both EC and dust, while at the same time there is a tendency for a reduction in the MAC value with snow depth. This work emphasizes the complexity in determining the snow albedo, showing that LAI concentrations alone might not be sufficient, but additional transient effects on the light-absorbing properties of the EC need to be considered and studied in the snow. Equally imperative is to confirm the spatial and temporal representativeness of these data by comparing data from several and longer pits explored at the same time.

1. **Introduction**

The deposition of light-absorbing impurities (LAI) in snow influences the radiation budget and can cause enhanced melting (Warren and Wiscombe, 1980). This process affects regions with seasonal snow cover, leading to an earlier snow retreat, which has major implications for thawing and biogeochemical processes acting in the ground (AMAP 2011). In mountainous areas with glaciers, the impurities perturb glacier properties and the hydrological cycle (e.g. Xu et al., 2009). In this context, the impact on snow reflectance (albedo) from black carbon (BC) aerosol particles is of particular interest. Being one of the most effective light-absorbing aerosols, BC enters the atmosphere by combustion of carbon-based fuels, including forest fires and anthropogenic burning of bio- and fossil fuels (Bond et al., 2013). Because of its negative effect on snow albedo, considerable effort has been made to globally quantify BC in snow (e.g. Doherty et al., 2010; Ming et al., 2008; Schmitt et al., 2015), as well as in ice cores (e.g. McConnell et al., 2007; Ruppel et al., 2014; Xu et al., 2009). In urban areas and in households using open fires, BC particles are also known to have adverse health effects, which make them interesting from a human health perspective as well (e.g. Shindell 2012).

The potential impact of LAI in snow and ice make the Himalaya a region of special interest. It contains numerous glaciers which are in a general state of recession, although contrasting patterns have been reported in different areas (e.g. Bolch et al., 2012; Kääb et al., 2012). Himalayan glaciers act as freshwater sources for several major rivers in Asia, including Indus, Ganges, Brahmaputra, Mekong, and Yangtze, thus having a vital part in millions of people's lives (e.g. Immerzeel et al., 2010). The glaciers are especially susceptible to BC emissions, since India and China located in close proximity, emit the most BC world-wide (Bond et al., 2007). A recent study by Ming et al. (2015) found a decreasing trend in albedo during the period of 2000-2011 on Himalayan glaciers, and suggested rising air temperatures and deposition of LAI to be responsible for the decrease. In light of the vast area of the Himalayas, there is a lack of in-situ measurements of LAI on glaciers, which are crucial for modeling work (Gertler et al., 2016). The lack of measurements is especially pronounced in the Indian Himalaya, since previous measurements of LAI in Himalayan snow and ice have largely been confined to China (e.g. Xu et al., 2006) and Nepal (e.g. Ginot et al., 2014; Kaspari et al., 2011; Kaspari et al., 2014; Ming et al., 2008).

At present, three primary methods are used to measure BC in snow and ice (see Qian et al., 2015, in which they are extensively presented). Out of the three methods, two utilize filters to collect impurities in a melted sample. The first filter method measures optically the spectrally resolved absorption by the impurities using an integrating sphere integrating sandwich spectrophotometer (ISSW) (e.g. Doherty et al., 2010; Grenfell et al., 2011). The second filter method is the thermal-optical analysis of filters (e.g. Forsström et al., 2009; Hagler et al., 2007). The third, non-filter-based method, uses laser-induced

1   incandescence with a single particle soot photometer (SP2) (e.g. McConnell et al., 2007; Schwarz et al.,

2   2012).

3   Each measurement method has benefits and drawbacks. The SP2 is specific to refractory BC and is able

4   to provide estimates on the size of the BC particles. However, the SP2 has a size range limitation

5   (roughly 70–600 nm, depending on the instrument settings and nebulizer settup), which may result in

6   the underestimation of BC mass since particles in snow have been reported to be larger (Schwarz et al.,

7   2012; Schwarz et al., 2013). Moreover, the SP2 technique needs to have the liquid particles aerosolized,

8   which may lead to additional particle losses (Schwarz et al., 2012). The use of filters, on the other hand,

9   can provide a practical logistics advantage for the collection of LAI in remote locations because it is

10   difficult to maintain the necessary frozen chain for the snow samples from the field to the laboratory

11   for analysis. Filtering of liquid samples can be conducted in the field, and the substrates are more easily

12   stored and transported to the laboratory. The ISSW method has the advantage that it measures light-

13   absorbing constituents on the filter indiscriminately. Thus, the ISSW method is not specific to BC, and

14   requires interpretation of the spectral response to determine the BC component. The thermal-optical

15   method (TOM) provides an actual measurement of elemental carbon (EC) that is instrumentally defined.

16   EC is assumed to be the dominant light-absorbing component of BC, and often EC and BC are used

17   interchangeably in literature. The sampling efficiency of quartz filters used in TOM is not well

18   characterized for small particles (Lim et al., 2014). However, smaller particles normally contribute little

19   to total particulate mass (Hinds 1999). Thus, each method for measuring BC in snow has both

20   advantages and disadvantages.

21   In addition to BC, other LAI may contribute significantly to the radiative balance of the cryosphere.

22   Recent research has identified mineral dust and microbiology as having a more important role than

23   previously thought in the current decline in albedo of the Greenland Ice sheet and other parts of the

24   Arctic (e.g. Dumont et al. 2014, Lutz et al., 2016). Similarly, Kaspari et al. (2014) reported such high

25   dust concentrations in the snow of Himalayan Nepal that the contribution of dust in lowering the snow

26   albedo sometimes exceeded that of BC. The importance of dust has also been illustrated from other

27   regions, for example the Colorado Rockies, US, where dust causes a significantly earlier peak in runoff

28   (Painter et al. 2007). In the Arctic, Doherty et al. (2010) suggest that 30 to 50 % of sunlight absorbed

29   in the snowpack by impurities is due to non-BC constituents. Evidently, dust has an important role in

30   the cryospheric radiative balance. Differentiating between the different impurities in the snow is not

31   trivial, however, and requires more than one analytical technique (Doherty et al., 2016). Traditionally,

32   dust in snow has been quantified by gravimetrically measuring filters (e.g. Aoki et al., 2006; Painter et

33   al., 2012). Other methods have consisted of using a transmitted light microscopy (Thevenon et al.,

34   2009), a microparticle counter to measure the insoluble dust (Ginot et al., 2014), or mass spectrometry

35   (using iron as a proxy for dust) (Kaspari et al., 2014).

1 Here we present observations of LAI in snow from two glaciers in the Sunderdhunga valley in Indian

2 Himalaya, which have not to our knowledge, been explored previously with respect to LAI in snow.

3 Using a measuring approach whereby the TOM is combined with a custom-built particle soot absorption

4 photometer (PSAP), we perform laboratory test to provide a correct interpretation of the results. Our

5 Himalayan observations are further compared to samples from Arctic Finland for their LAI content.

6 **2. Methodology**

7 **2.1 Snow sample collection and site characteristics**

8 *2.1.1 Himalayan India*

9 Snow samples were collected in September of 2015, during the Indian post-monsoon season, from two

10 adjacent glaciers in the Sunderdhunga valley (Figure 1). Bhanolti and Durga Kot glaciers (N 30º 12', E

11 79º 51') are located in the state of Uttarakhand, India. Facing northeast the glaciers cover an elevation

12 range of about 4400-5500 m a.s.l. and are two small valley-type glaciers contributing to the Ganges

13 hydrological basin. Since the glaciers are situated at a relatively low altitude, they are more likely to be

14 exposed to BC than other Himalayan glaciers residing in higher altitude, as BC has been shown to

15 decrease with altitude in other parts of the Himalaya (e.g. Kaspari et al., 2014; Ming et al., 2013; Yang

16 et al., 2015). The Sunderdhunga area does not have any major local pollution sources. Regionally,

17 however, the small towns of Bageshwar (~40 km S; population ~9000) and Almora (~70 km S;

18 population ~34000), may play a role. On a larger scale, the Sunderdhunga area is affected by the large-

19 scale emissions from the Indo-Gangetic Plain (IGP). Measurements of airborne BC and other aerosol

20 particles at Mukteshwar, a distance of ~90 km southwards at an altitude of 2200 m a.s.l., have shown a

21 clear seasonal pattern in atmospheric concentrations with emissions originating from the IGP

22 (Hyvärinen et al., 2011; Raatikainen et al., 2017). With a peak during the pre-monsoon season (March-

23 onset of monsoon), the BC loading has been reported to decrease by about 70 % at Mukteshwar during

24 the monsoon (Hyvärinen et al., 2011). Similarly, dust concentrations in the air have been shown to peak

25 during the pre-monsoon season at Mukteshwar (Hyvärinen et al., 2011). The pre-monsoon season, also

26 known as the "dust-season" in India, brings air masses from the Thar Desert transporting dust to the

27 Himalaya (Gautam et al., 2013). Dust from local sources have also been identified at Mukteshwar

28 during this season (Hyvärinen et al., 2011).

29 At Durga Kot glacier four snow pits with varying depths were dug at different elevations, while at

30 Bhanolti glacier one snow pit was dug (see table 1 for snow pits and sample details). Snow samples

31 were collected with a metal spatula in Nasco whirl-pak bags, and thereafter brought to the designated

32 base camp where the snow was melted and filtered. Since it was not possible to maintain the crucial

33 frozen chain for the snow samples during transport back to the laboratory this approach of melting in

34 the field was used for the glacier snow samples. The snow was melted gently over a camping stove in

1 protected glassware to avoid contamination. The liquid samples were subsequently filtered through

2 quartz fiber filters (Munktell, 55 mm, grade T 293), in accordance to previous work (e.g. Forsström et

3 al., 2009; Svensson et al., 2013). The dried filters were then transported in petri dishes to the laboratory

4 for analysis (described in section 2.2).
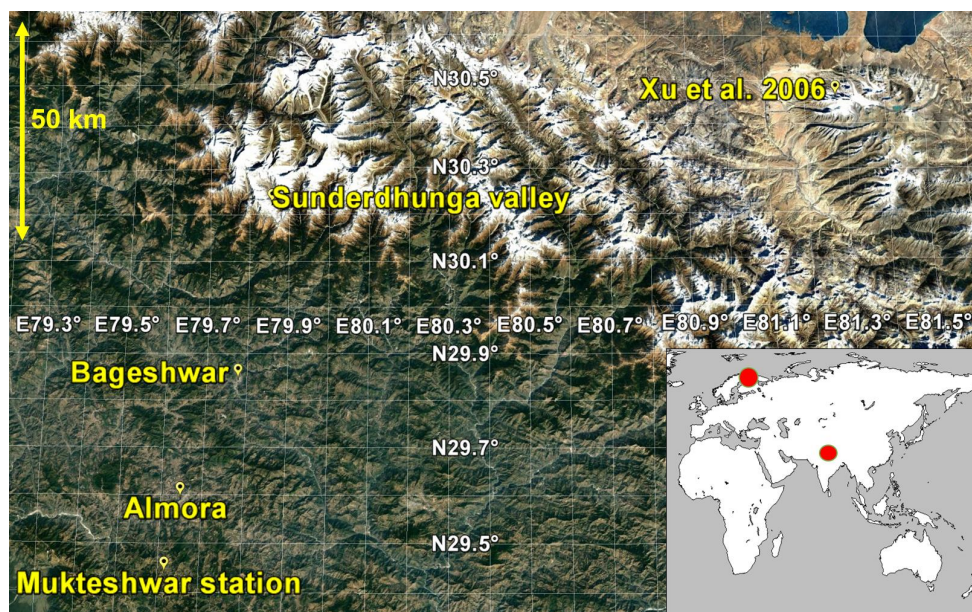
6 Figure 1. Google earth image of Indian sampling location, with sites discussed in text, as well as an

7 overview map of measurement sites.

8 *2.1.2 Arctic Finland*

9 Snow samples collected in Finland originated from the seasonal snowpack of Sodankylä (N 67º 21' E

10 26º 37') and Pallas (N 67º 58' E 24º 06') c.f. Figure 1. The Pallas samples were gathered in March and

11 April of 2015 (n=10) from an open mire and in March of 2016 (n=2) from an area above the tree line

12 (in close proximity of the Pallas Global Atmosphere Watch Station). More details of the Pallas sampling

13 area are provided in Svensson et al. (2013) where EC in the snow was previously investigated. The

14 snow sampled was confined to the top layers of the snowpack. The Sodankylä samples (n=15) are from

15 the Finnish Meteorological Institute Arctic Research Center, where weekly surface snow samples (0-5

16 cm) have been collected since 2009 (first part of time series is presented in Meinander et al., 2013;

17 where details of area are provided). The samples used in this study originate from spring of 2013 and

18 2014. The snow samples from Pallas and Sodankylä were collected in Nasco whirl-pak bags and stored

19 in a frozen state until filtration. Samples were then melted in a microwave oven at each site's respective

1 laboratory, and followed the same filtering procedure described above, according to e.g. Forsström et

2 al. (2009) and Svensson et al. (2013).

3 **2.2 Light-absorbing impurities analysis**

4 To estimate the contribution to the reduction in transmission on the filter sample substrate due to

5 minerals, we compared the light transmission through the filter using the PSAP before and after heating

6 the sample as part of the TOM analysis. Since it is difficult to gravimetrically determine the dust content

7 on quartz filters, we decided to use this combined instrument approach to estimate the dust content. A

8 custom built PSAP (Krecl et al., 2007) was used for the optical measurements, and for the TOM a

9 Sunset Laboratory OCEC-analyzer was used to determine EC. A brief description of the OCEC-

10 analyzer and the PSAP is given below in sections 2.2.1 and 2.2.2, respectively.

11 The approach of measuring light transmission before and after heat treatment to estimate the different

12 light-absorbing components has been previously used for airborne sampled aerosol (e.g. Hansen et al.,

13 1993). In Hansen et al. (1993), filter samples were optically analyzed before and after being treated in

14 a 600°C furnace, in which the carbonaceous material was vaporized from the filter. These measurements

15 enabled them to obtain an estimate of the dust content on the filter. Lavanchy et al. (1999) followed a

16 similar optical and thermal approach to determine the BC and dust content of ice core samples. For the

17 EC measurement they used a two-step combustion procedure by Cachier et al. (1989), and in between

18 the thermal treatment they used a modified version of an aethalometer to measure the attenuation of

19 light through the filter. Our experimental method is analogous to that of Lavanchy et al. (1999).

20 However, as a Sunset Lab. OCEC-analyzer and a custom built PSAP were readily available to us, this

21 instrument configuration was used in our study. Because results from this type of analysis may be very

22 instrument specific, a series of laboratory tests (described in section 2.3) were conducted to confirm

23 reliability of the method before ambient snow samples were measured. The analysis procedure for the

24 filters (outlined further in section 2.3) was the same for the laboratory samples and the ambient samples.

25 *2.2.1 Elemental carbon analysis*

26 From a 10 cm^2 filter sample area, separate punches of 1 cm^2 were taken and analyzed for organic carbon

27 (OC) and EC content using a Sunset laboratory OCEC-analyzer (Birch and Cary, 1996) with the

28 EUSAAR_2 analysis protocol (Cavalli et al., 2010). First, in a helium atmosphere, the filter punch is

29 heated at different temperature steps. In this phase OC is volatilized and detected by a flame ionization

30 detector (FID). During the second stage, oxygen is introduced, and EC is released from the filter through

31 combustion. To account for pyrolysis occurring (darkening of the filter) during the first step, a laser (at

32 a 632 nm wavelength) measures the transmittance (or reflectance as an option for newer instruments)

33 continuously of the filter punch, and when the original value of the transmittance is attained during the

34 second step separation between OC and EC is done. The filters EC values reported here (referred to as

1   EC_{TOM}) are based on the transmittance correction for pyrolysis since the PSAP operates also on the

2   basis of transmittance through the substrate. An additional EC value provided by the OCEC-analyzer

3   from the analysis is an optical EC ($EC_{optical}$), which is based on the monitored transmittance and

4   absorption coefficients of the OCEC-analyzer. For this study no special consideration was taken for

5   carbon carbonate particles that can be present in the sample (Chow & Watson, 2002). Unless chemically

6   removed before analysis, these particles will contribute to the OC fraction of the total particulate carbon

7   content (e.g. Cavalli et al., 2010).

8   Uncertainties associated with the TOM method are mainly associated with the inefficiency of the filters

9   to capture the small impurities, uneven filter loading, and loss of particles to filtering containers

10   (Forsström et al., 2013). The artifact from samples with a high fraction of pyrolysis OC (Lim et al.,

11   2014), and the interference of an accurate split point determination from filters containing a high dust

12   load can also be considerable (Wang et al., 2012).

13   *2.2.2 Absorption measurements*

14   The PSAP use a single diode at 526 nm as light source. The light is split by two light pipes which

15   illuminate two areas of 3.1 mm in diameter. The filter substrate is placed over these areas and individual

16   detectors below the filter measure the transmitted light. During normal operations, when measuring BC

17   in air, these two signals are used as sample and reference spots. The reference spot is exposed to particle

18   free air and the sample spot is exposed to particles present in the ambient air. In this experiment both

19   signals are used to measure the change in transmission by comparing the signal before and after the

20   filter has been analyzed using TOM. The signal change is related to the transmission from a particle

21   free filter (filtered using Milli-Q (MQ) water and dried).

22   The corrections required for the PSAP when used for air sampling is well documented (e.g. Bond et al.,

23   1999; Virkkula et al., 2005), in particular this concerns enhanced absorption from the filter itself through

24   multiple scattering effects from the filter fibers, and particle loading effects (shadowing and reduction

25   in multiple scattering). However, these corrections are essentially uncharacterized for melted snow

26   samples and the quartz fiber filters used. The fiber filters used are substantially thicker compared to

27   what is normally used for PSAP measurements (Pallflex cellulose membrane filter) or the ISSW

28   measurements (Nuclepore filter). Moreover, the filter substrate is very large in terms of surface area

29   compared to the particles sampled. The geometry is very complex and in relation to a particle the

30   substrate is more of a three dimensional web or sponge rather than a flat surface area on a filter. An

31   example of a blank filter sample obtained by a scanning electron microscope is presented in Figure 2.

32   The horizontal scale of 500 mm is for comparison, and the scale of 150 mm is to illustrate the relative

33   thickness of the substrate.
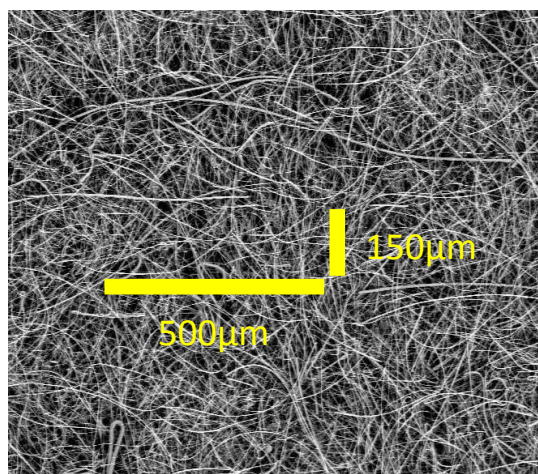
2   Figure 2. Electron microscope image of a blank quartz fiber filter used in this study.

3   The basis for the optical attenuation measurements is the exponential attenuation of light as it passes

4   through some medium, often described by the Bouguer-Lambert-Beer-law (Eq. 1).

5                                    $I = I_0\, e^{-\tau}$,   (Eq. 1)

6   where I_0 in our case is the light intensity through a clean filter and, I is the light intensity through a

7   sample loaded filter. The exponent τ is the optical depth of LAI on the filter. For our study the multiple

8   scattering absorption enhancement factor of the filter will be treated as a constant, but not given a

9   numerical value. Due to the geometry of the filter, corrections for any enhanced absorption due to co-

10   existing scattering particles, and the loading effect, are not specifically considered. Hence, we will

11   assume a linear relation between the logarithmic change in transmittance (T_r) of a filter and the optical

12   depth (Eq. 2).

13                                    $ln(T_r) = \tau_{TOT}$, (Eq. 2)

14   where $T_r = \frac{I_0}{I}$ and τ_{TOT} is the combined effect of all light absorbing impurities. Our interest was to

15   estimate the relative contributions of EC (τ_{EC},) and mineral dust (τ_D) particles to measured optical depth

16   according to equation 3.

17                                    $\tau_{TOT} = \tau_{EC} + \tau_D$, (Eq. 3)

18   From TOM we get the EC mass surface density (µg cm^{-2}). Thus, we can write τ_{EC} as the product of the

19   EC mass surface density on the filter and an effective material specific mass absorption cross section

20   MAC$_{eff,EC}$ of BC that includes the multiple scattering enhancement of the filter. Typically, MAC values

21   are reported in units of m^2 g^{-1}.

1   **2.3 Laboratory tests**

2   Before initiating analysis of the field samples, a series of laboratory tests using the OCEC-analyzer and

3   the PSAP combination were conducted. For this purpose, the following filter sets were created:

4   1. A set of filter samples (n=36) with different amounts of BC. Two types of soot (BC) were used

5   and each was mixed (a minute amount of soot not weighed) with MQ water and a small amount

6   of ethanol (to enable mixing of the BC particles in the liquid) in an ultra-sonic bath. One soot

7   type was collected by chimney cleaners in Helsinki, Finland, originating from oil-based

8   combustion, and has been used previously in soot on snow experiments (Svensson et al., 2016).

9   The second type was a product from NIST (National Institute of Standards and Technology),

10   which consists of diesel particle matter from industrial forklifts, NIST-2975. From the BC stock

11   solutions, different amounts of solution were taken out and diluted with additional water for the

12   same total volume of filtrate (ca. 0.5 L liquid). The newly created mixture solution was

13   thereafter filtered using the same filter procedure as the ambient snow samples (described in

14   2.1.1).

15   2. The second set of filters (n=16) generated contained mineral dust only. Analogous to the soot

16   mixtures, two types of mineral were used. The first mineral was SiC, Carborundum, mesh nr.

17   1200, corresponding to particles approximately < 1 µm in diameter. The amount of SiC added

18   to the MQ water was measured using a digital scale (resolution of 10 µg) before filtration. With

19   the known concentration of the mixture, we observed how much of the weighed mineral was

20   deposited on the filter during filtration to estimate losses. By comparing the whole filters before

21   and after filtration gravimetrically, these tests showed that 10 % or less of the mineral was lost

22   during filtering. The second type of mineral consisted of stone crush from a site in Stockholm,

23   Ulriksdal, likely to be mainly granite. A sieve mesh nr. of 400 was used for this material, which

24   corresponds to mineral particles of approximately < 38 µm in diameter. Filters were prepared

25   according to the procedure given above for the other mineral (SiC).

26   3. The last set of laboratory solutions made contained various mixtures of SiC mineral and

27   chimney soot (n=30). These filters were treated in the same way as described above, with a soot

28   stock solution and a mineral weighed solution being mixed into one solution.

29   The procedure to analyze all three sets of filters samples was identical. After the filter substrates had

30   dried, one punch (1 cm^2) from the filter was put into the PSAP instrument to measure the transmission

31   across the filter in relation to a blank filter. This punch was taken for analyses of OC and EC content

32   using the OCEC-analyzer. After the TOM, and removal of the carbonaceous particles, this filter punch

33   was again analyzed in the PSAP. Hence, we acquired the transmission through the filter before heating

34   and after heating in comparison to a blank filter. We did tests where the same filter punch was used in

35   the PSAP instrument as well as the OCEC-analyzer, and compared this to twin samples that were used

1   in separate instruments. Both procedures provided the same result. Furthermore, extensive tests were

2   carried out using blank filters that had been subject to filtering of MQ water and treated the same way

3   as prepared samples and the ambient snow samples. No measurable EC could be detected on these

4   filters. It should be noted that part of the second set of the laboratory filters (stone crush mineral) were

5   analyzed with a different, but identical, PSAP and OCEC-analyzer at a different laboratory (Stockholm

6   University).

7   **3.   Results and discussion**

8   **3.1 Laboratory samples**

9   The change in optical depth as a function of analyzed EC using our two standard types of BC particles

10   (filter set nr. 1) is shown in Figure 3. Both materials behave optically similar and the slopes are within

11   15 % of each other, with chimney soot having a slope of $39.8 \pm 1.5 \ m^2 \ g^{-1}$ and NIST soot $34.4 \pm 1.8 \ m^2$

12   g^{-1} (fits have been set to a fixed intercept at 0; $\pm$ refers to standard error of slope). Previous studies of

13   atmospheric airborne BC aerosol and its MAC with different filter-based absorption photometers are

14   numerous, while reported MAC values for BC in snow are very sparse. The MAC value of BC is

15   dependent of many factors, such as particle size, density, and refractive index, mixing state (i.e.

16   coating), thus many influences on it. Reported airborne BC MAC values are lower than what we found

17   for the two soot standards (which were mixed in liquid solution to simulate similar conditions as for our

18   ambient snow samples). However, the MAC of air sample usually takes into account the multiple-

19   scattering correction factor (C_{ref}). For example for the commonly used aethalometer, its optical depth is

20   divided by a C_{ref} somewhere in the range of 2.8-4.3 (Collaud Coen et al., 2010). If a C_{ref} of 5.2 was

21   considered for our liquid originating BC data, similar MAC values would be found (e.g. Bond et al.

22   (2013) reports freshly-generated BC with a MAC of $7.5 \pm 1.2 \ m^2 \ g^{-1}$ at $\lambda = 550$ nm). However, for our

23   data set we have chosen not to take any C_{ref} into account as our samples are liquid instead of air based,

24   and currently no C_{ref} exists for liquid samples.
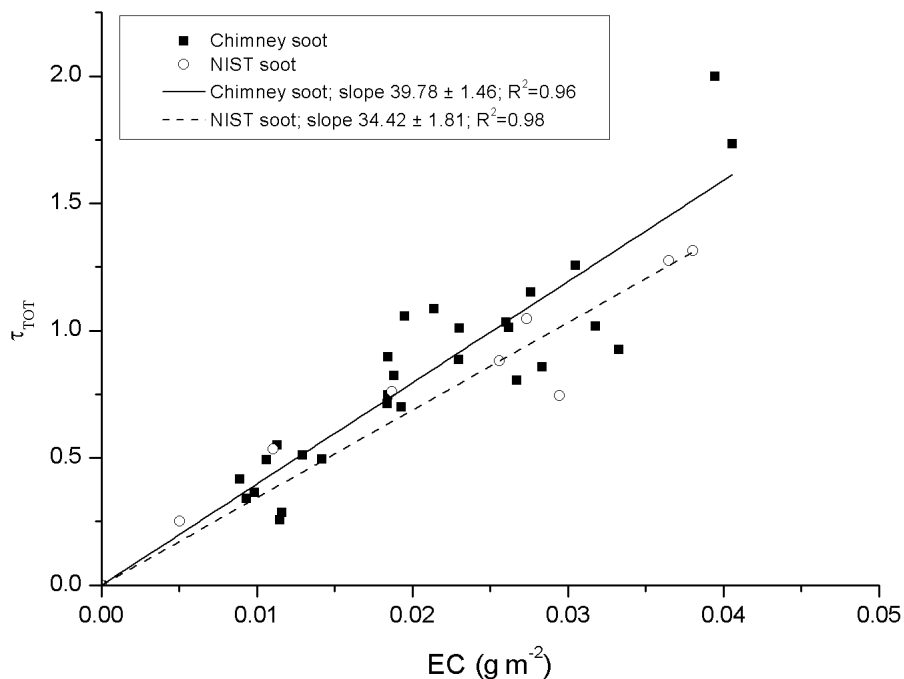
Figure 3. Comparison between the optical depth (at λ=526 nm) by Chimney and NIST soot as function

of analyzed EC density by the OCEC-analyzer.

Figure 4 shows the analogous results as in Figure 3, but for the two mineral aerosol solutions (filter set

nr. 2). The slope of the optical depth of SiC versus measured SiC amount is more than a factor of one

hundred smaller (0.23 ± 0.008 m^2 g^{-1}) than the slopes for our BC standards. This is consistent with

previously reported results for airborne mineral dust (e.g. Hansen et al., 1993). The stone crush material,

an essentially white powder, yielded an even smaller slope of 0.02 ± 0.001 m^2 g^{-1}. Clearly, the slopes,

or the MAC, for the mineral particles are very composition specific. For a few (n=5) of the mineral

aerosol samples the optical depth was measured both before and after TOM. No EC was detected on

these samples and no significant difference in τ could be observed before and after heating the sample,

as one would expect since no BC was added to these filters.
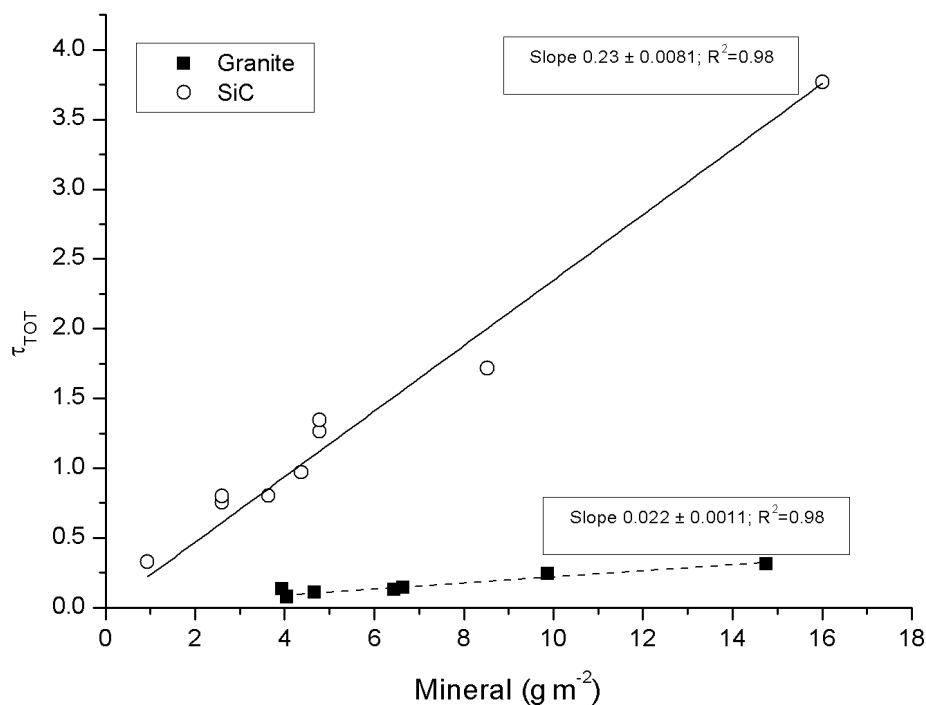
2   Figure 4. The optical depth as a function of the amount of minerals present on the filter.

3   From the analysis of chimney and NIST soot (Fig. 3) and SiC and stone crush dust (Fig. 4) the

4   experiments were extended to comprise mixtures of soot and dust. Using the MAC of chimney soot

5   (see Fig. 3), we estimate the EC content of the third set of filters, containing a mixture of SiC and

6   chimney soot. The estimated EC (eEC) is based on the difference between the optical thickness before

7   TOM analysis (τ_{TOT}) and the optical thickness after the analysis (τ_D). eEC is then compared to the

8   amount of EC obtained in TOM, for the same filters. This comparison is presented in Figure 5. The data

9   is rather scattered, but the slope of the linear regression is relatively close (17 %) to 1:1. Hence it shows

10   that EC can be reproduced reasonably well based on the PSAP measurement even for a mixture of BC

11   and minerals.
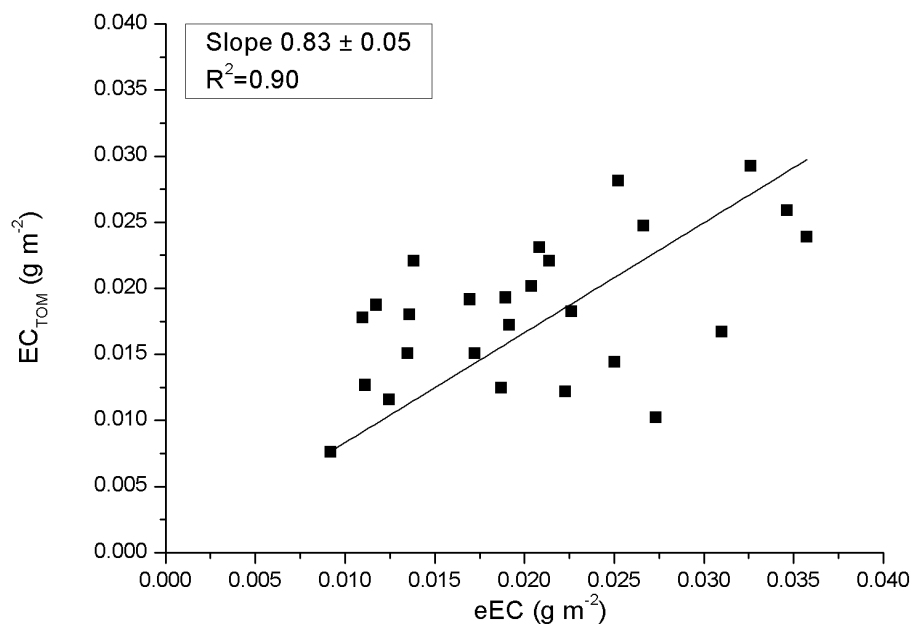
2   Figure 5. EC amount observed by the TOM (EC$_{TOM}$) for Chimney soot and SiC mixtures as a function

3   of estimated EC (eEC), using a PSAP optical depth signal before and after heating the filter and using

4   the MAC$_{eff,EC}$ of 39.8 m^2 g^{-1} from Figure 3.

5   In the context of this work it is further useful to compare our eEC content with the optical EC reported

6   by the OCEC-analyzer. This comparison is presented in Figure 6, again for the third set of filters

7   (Chimney soot+SiC). As observed, the two optically different derived EC amounts show a very

8   consistent relation with nearly a slope of one. The good agreement between the two optically derived

9   EC values suggests that much of the scatter seen in Figure 5 is due to the uncertainty in the analyzed

10   content of EC using TOM (and FID).
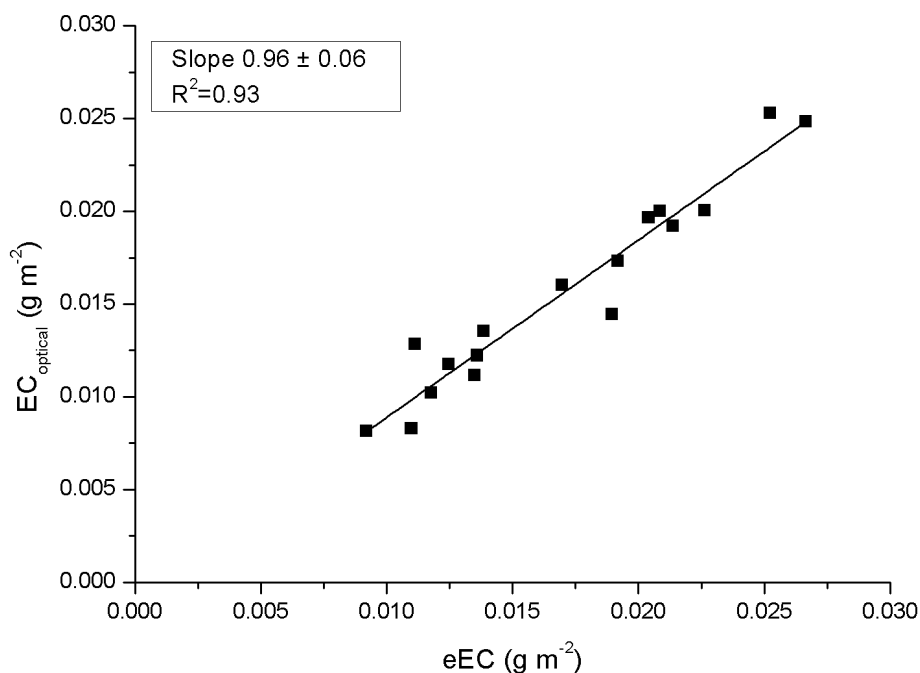
2 Figure 6. Comparison between the optically reported EC by the OCEC-analyzer and the derived EC

3 surface amount on the substrate (using PSAP data and the relation in Figure 3). The data is for filters

4 containing mixtures of Chimney soot and SiC.

5 In addition to chimney soot, the mineral SiC is the second absorbing component on the third set of

6 filters. In Figure 7 the optically estimated SiC content, based on the SiC slope in Figure 4 and τ_D is

7 compared to the known weighed amount of SiC before adding it to the liquid. Similarly, as in Figure 5,

8 there is some scatter in the data, but the overall pattern indicates a consistency with a reliable optical

9 measurement. There are two slopes presented, one including all of the data points (slope 1.02), and the

10 second slope (0.88) excluding three data points with weighed SiC amounts exceeding 7.5 g m^{-2}.
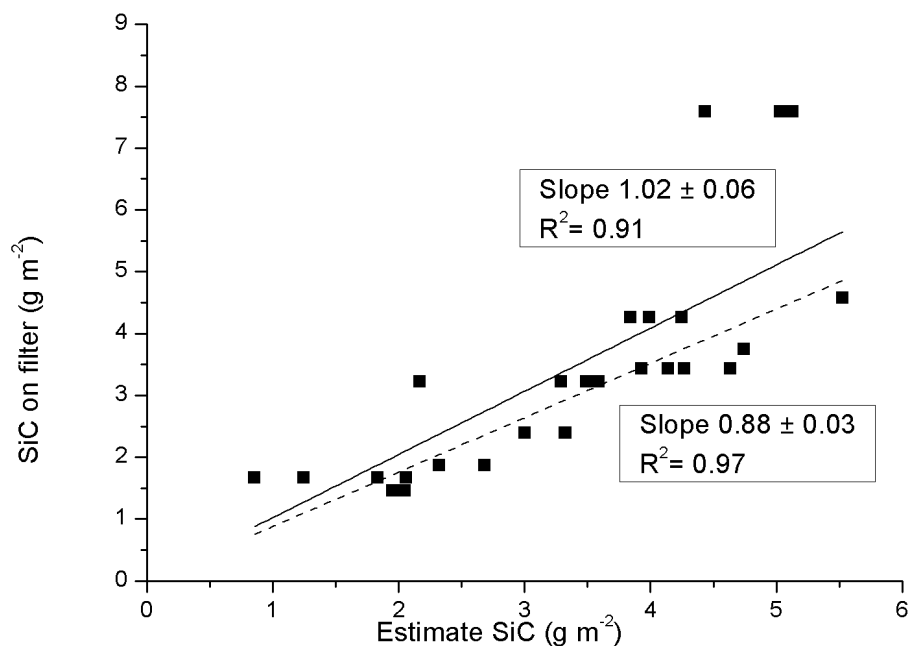
2   Figure 7. Comparison between the weighed SiC amounts added to the water and the optically derived

3   SiC density on the substrate. The data is for Chimney soot and SiC mixtures, with two alternative slopes;

4   one contain all data points (1.02), and one excluding three data point in the top right of graph (0.88).

5   Based on the relations established for EC and SiC individually in figures 3 and 4, respectively, it is

6   possible to retrieve their separate concentrations from a mixture based on the change in filter

7   transmission before and after heating the filter. The consistent results from these laboratory tests gives

8   confidence in applying this method on our ambient samples from India and Finland.

9   **3.2 Ambient snow samples**

10   *3.2.1 EC in snow*

11   In all of the snow pits from Sunderdhunga a distinct layer with concentrated impurities was observed.

12   These impurity layers always had the highest EC concentrations (exceeding 300 µg L^{-1}) of each pit

13   (Table 1). For some of the samples from Sunderdhunga taken from the impurity concentrated layers,

14   the substrates were actually too loaded with material that quantitative impurity values could not be

15   determined (by not having an initial transmission value). Excluding these heavy impurity layers, the

16   average and median EC concentration for the other snow samples were 141.3 and 101.9 µg L^{-1},

17   respectively. Surface samples taken above 4900 m a.s.l. had EC concentrations in the range of 13.2-

1   65.7 µg L^{-1}. Consisting of relatively fresh snow, fallen during the previous days (or weeks), these

2   surface samples LAI content is likely to originate from the post-monsoon season.

3   Previous studies on BC in snow and ice from the Himalaya have shown seasonal variation. At Mera

4   glacier in Nepal Ginot et al. (2014) showed that BC concentrations peak during the pre-monsoon in a

5   shallow ice core. From the same glacier, Kaspari et al. (2014) observed similar seasonal peaks in BC

6   concentration in snow and firn samples taken above the equilibrium line altitude, where the snow had

7   not undergone any significant summer melt. Noteworthy, dust did not show the same strong seasonality

8   as BC in their studies (Ginot et al., 2014; Kaspari et al., 2014).

9   Measurements of BC in snow taken closest to Sunderdhunga, reported in the literature, are from about

10   140 km east-north-east (78º heading), at a higher altitude between 5780-6080 m a.s.l. Gathered in the

11   surface snow of Namunani glacier Xu et al. (2006) reported low EC concentrations in the range of 0.3-

12   9.7 ng g^{-1}. The difference between Sunderdhunga and Namunani can probably be attributed to the

13   difference in sampling altitude and different measurement techniques to determine the EC (Xu et al.

14   used a two-step heating-gas chromatography, similar to method of Lavanchy et al.). The difference

15   could also possibly be explained by the geographical location, with Namunani located on the northern

16   flank of the Himalaya, and it is on the leeward side of the main sources of LAI to the south. Furthermore,

17   it is not explicitly stated in Xu et al. during which season snow samples were collected, which likewise

18   would affect EC concentrations.

19   For reference in relation to the comparison of the dust signal below in 3.2.2, the EC concentrations in

20   the surface snow from the Finnish Arctic were in the range of 6.2-102 µg L^{-1}. Samples from Pallas had

21   an average and median of 40.0 and 31.0 µg L^{-1}, respectively, whereas the samples from Sodankylä had

22   an average of 23.7 µg L^{-1} and median of 13.1 µg L^{-1}. The higher concentration observed in Pallas is

23   likely because a majority of the samples originated from later in the snow season compared to

24   Sodankylä samples and EC has concentrated in the surface snow later in the season (e.g. Svensson et

25   al., 2013). On a broader scale the concentrations are in the same magnitude as previous measurements

26   of EC in snow (Forsström et al., 2013; Meinander et al., 2013; Svensson et al., 2013)

27   Our snow samples EC content is further compared in Figure 8, where the estimated EC content based

28   on the optical depth measurement is plotted against the optical EC output from the OCEC-analyzer. The

29   snow data presented in Figure 8 indicate the same relation between the two optical methods as presented

30   in Figure 6 for the standard soot. That is, slopes near 1:1 line, namely 1.19, 1.02, and 1.11 for

31   Sunderdhunga, Pallas, and Sodankylä samples, respectively. Hence, there is a strong consistency

32   between the two optical approaches in the interpretation of the change in τ before and after the substrate

33   has been analyzed with the EUSAAR-2 thermal protocol.
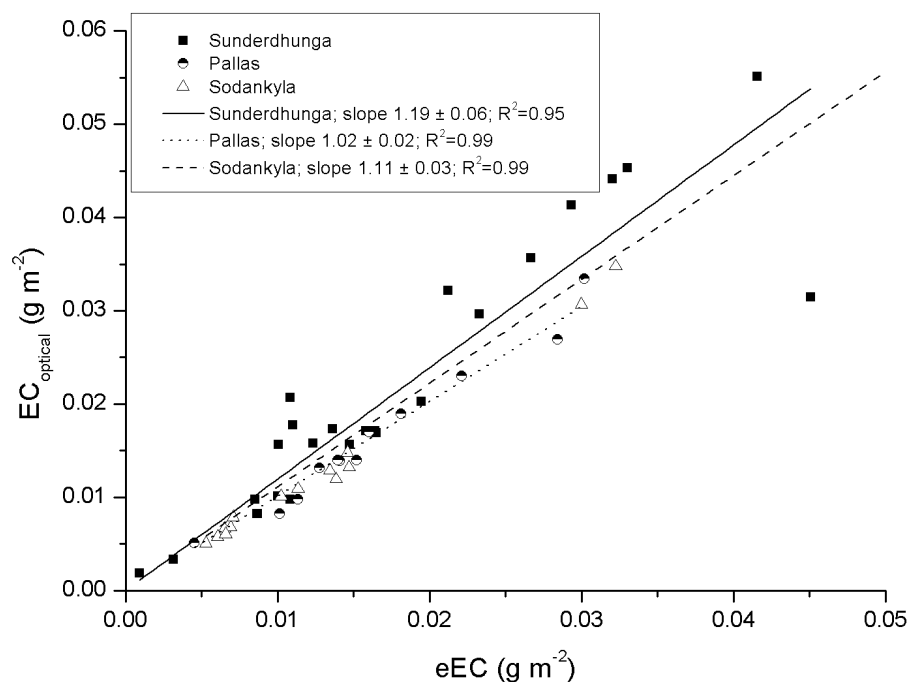
2   Figure 8. Comparison between the optical EC content given by the OCEC-analyzer and estimated EC

3   (eEC) content using a PSAP and a $MAC_{eff,EC}$ of 39.8 m^2 g^{-1}, for the Arctic and Himalayan samples.

4   Although the EC content determined by the optical method of the TOM and the eEC content based on

5   the PSAP and a MAC value (Figure 3) agree well, there is a significant difference in the site specific

6   derived MAC values. In Figure 9 the optical depth of EC (τ_{EC}) is plotted as a function of the analyzed

7   EC (with TOM) for all of the snow samples. The slopes for the three sampling sites are 21.0, 21.9 and

8   17.1 m^2 g^{-1} (Pallas, Sodankylä, and Sunderdhunga, respectively). These values are around half of what

9   the laboratory standard BC tests show (Fig. 3), indicating less absorbing efficiency for the EC particles

10   originating from the snow compared to the laboratory particles. This is unexpected, as any non-EC

11   absorbing material or even scattering particles mixed with EC would tend to increase the MAC value

12   compared to pure BC particles which we would expect to occur for our snow originating EC particles.

13   A consequence of a lower MAC for the snow EC particles could be that the snow albedo reduction

14   caused by the EC is inaccurate since the EC particles have less absorbing efficiency. Schwarz et al.

15   (2013) previously reported a lower MAC value for BC particles in the snow compared to airborne BC

16   particles due to a difference in mean size. The BC particles from the snow were observed to be larger

17   compared to airborne BC particles, explaining the decrease in MAC for the snow originating particles.

1   The authors further showed how the BC effect in snow albedo reduction is currently overestimated due

2   to the lower MAC for snow BC particles.
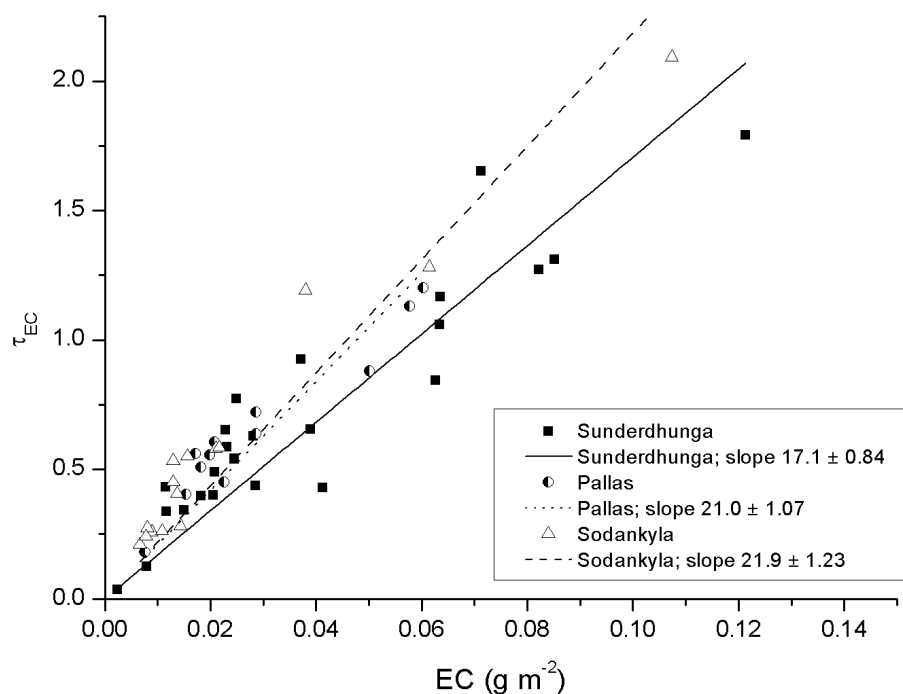
4   Figure 9. The optical depth τ_{EC} as function of the analyzed EC based on TOM, for the Arctic and

5   Himalayan samples.

6   In our case, if the laboratory generated BC consist of smaller particles compared to the snow samples

7   this could lead to a larger MAC value for the lab-standards. The size distribution of the BC particles in

8   the filters are unknown to us, but as suggested by the modelled MAC curve, presented in Figure 10, this

9   size dependence can play a role. The modelled MAC for theoretical BC particles demonstrate a decrease

10   in MAC with particle size, particularly for particles larger than about 130 nm. The absorption

11   efficiencies were calculated for $\lambda = 526$ nm by using the Mie code of Barber and Hill (1990) and for

12   BC the same complex refractive index of 1.85 - 0.71i that was used by Lack and Cappa (2010) and a

13   particle density of 1.7 g cm^{-3}.
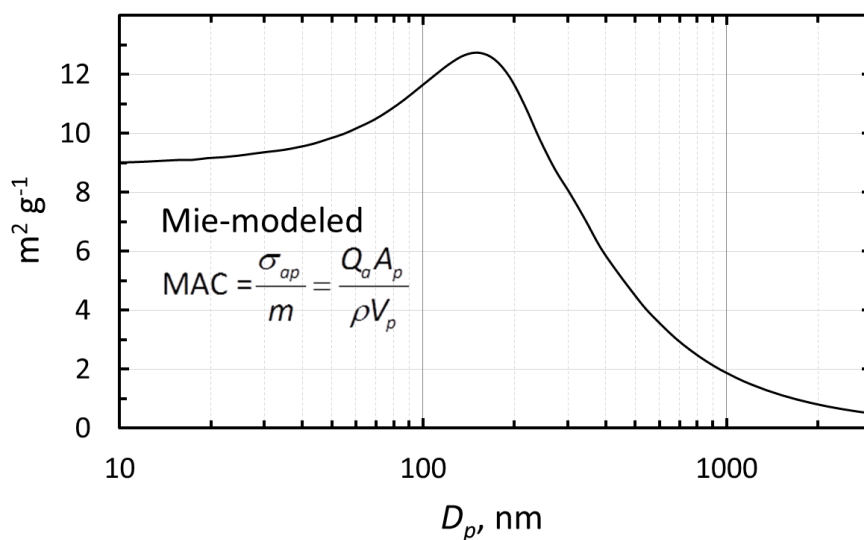
2 Figure 10. Modeled mass absorption coefficient (MAC) of single BC particles as a function of particle

3 diameter at $\lambda = 526$ nm.

4 Another hypothesis is related to the fact that the samples are liquids and that the matrix is strongly light

5 scattering and rather thick. It is likely that the liquid will embed the particles deeper into the filter than

6 what is typical for air samples (e.g. Chen et al., 2004). In air and on filter surfaces, BC mixed with a

7 scattering medium enhance the absorption. On the samples presented in Table 1, about 90 to 95% of

8 the carbon is water insoluble organic carbon, whereas the laboratory BC were essentially free from OC.

9 This difference could explain the lower MAC for the ambient samples if the net effect of the added OC

10 actually made the BC less efficient absorber in this particular matrix. Further tests are required,

11 however, to confirm this hypothesis.

12 *3.2.2 Dust fraction of LAI in snow*

13 Because the ambient mineral dust MAC value is unknown for our snow samples, it is not applicable to

14 use the SiC or stone crush MAC values to estimate the dust content on the filters. Instead, we use the

15 fraction of minerals (f_D) expressed in percent of the total optical thickness, $\left(\frac{\tau_D}{\tau_{TOT}} \ 100 \ \% \right)$ to estimate

16 the mineral aerosol contribution to the filter absorption. In our data set, there is a systematic difference

17 between the two Arctic sites and the Himalaya site (Fig. 11). For Pallas and Sodankylä f_D is typically

18 less than 20 %, whereas for Sunderdhunga f_D is typically much greater than that, with peaking fractions

19 reached at both ca. 35 and 65 %. For the Arctic, the values are broadly in line with previous estimates

20 on the amount of light absorption caused by other LAI than BC, i.e. 30-50 % (e.g. Doherty et al., 2010).

1   Studies from the Nepalese Himalaya concluded that dust may be responsible for about 40 % of the snow

2   albedo reduction (Kaspari et al., 2014). Similarly, Qu et al. (2014) observed that the contribution of dust

3   to albedo reduction can reach as high as 56 % on a glacier on the Tibetan plateau. Our dust estimate, as

4   a fraction of the LAI on the filter, shows similar results or an even greater fraction of dust than these

5   previous studies, highlighting the importance of dust (see also Fig. 12A) causing an albedo reduction

6   in this region of the Himalaya.
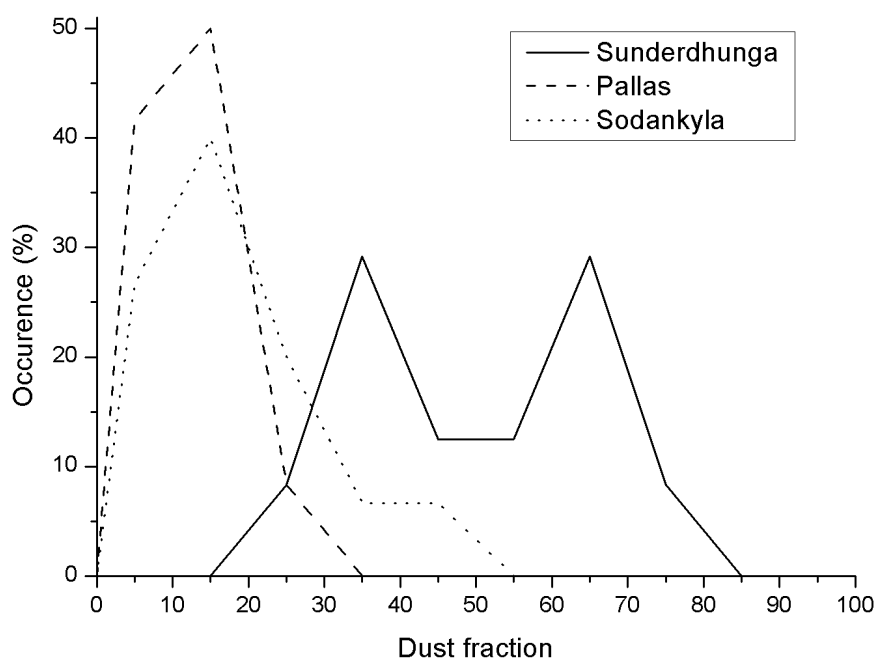
8   Figure 11. Frequency of occurrence for different derived dust fractions, f_D.

9   *3.2.3   Vertical distribution of LAI in Sunderdhunga*

10   A composite of the vertical profiles from pits C, D, and E are presented for EC and f_D in Figure 12A.
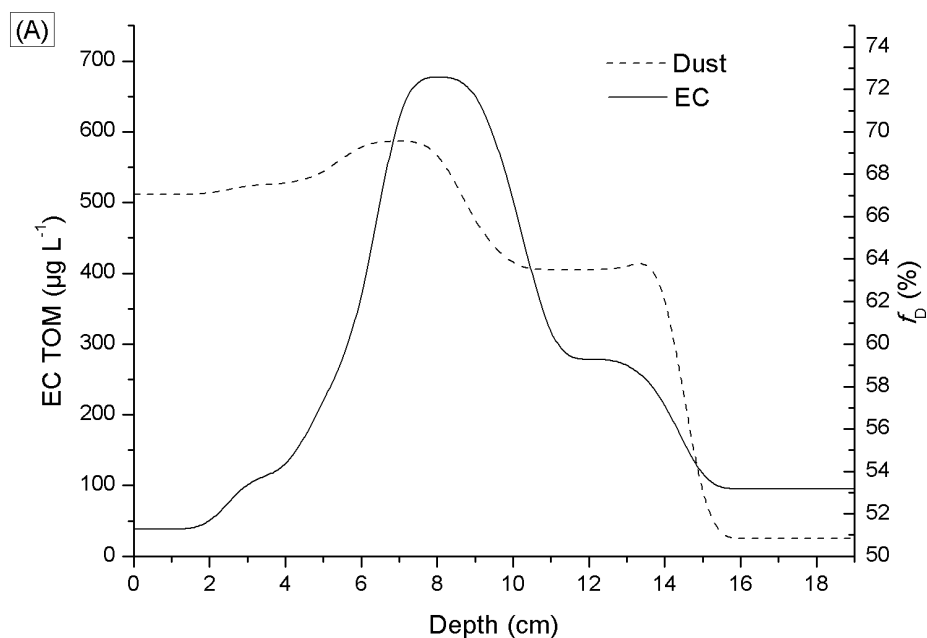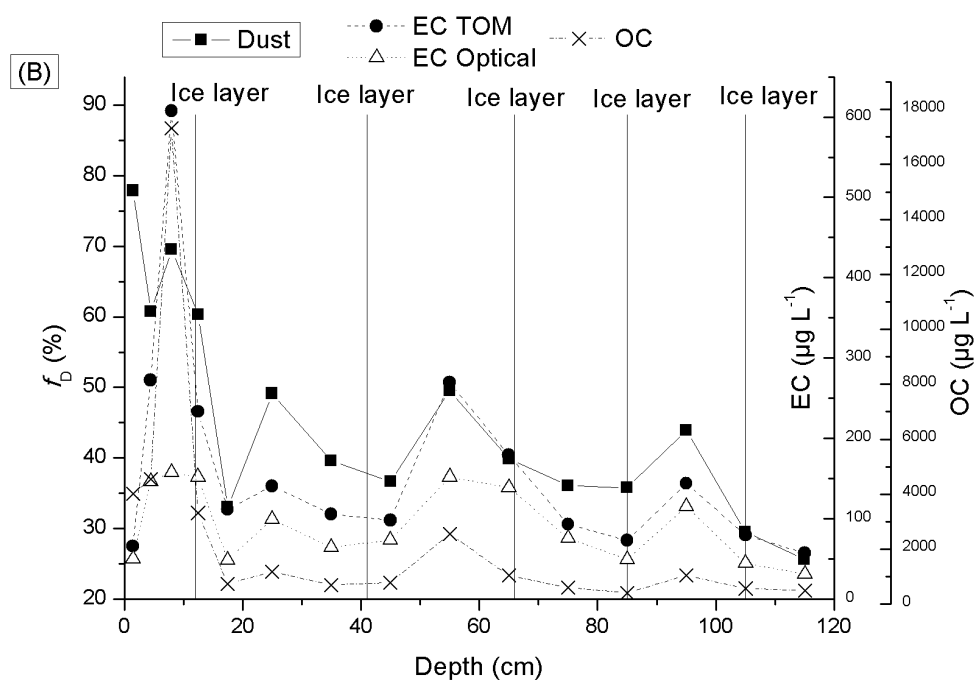
3 Figure 12. (A) Profile displaying average EC concentration and dust fraction from snow pits C and D

4 (Durga Kot glacier), and snow pit E (Bhanolti glacier); (B) Complete vertical profile E, taken at

5 Bhanolti glacier.

1   The variables plotted in Figure 12B display layers of enhanced amounts of both dust and EC, located

2   between ice layers, and additionally evidently high values at the top of the core above the first ice layer.

3   These layers are interpreted as indicators for seasonal variation at this location, with altering melt and

4   refreezing periods marked by the ice layers. Since the ice layers and the enhancements in LAI are

5   interleaved it suggest that the impurities were deposited on the glacier mainly in-between the melt and

6   refreeze periods. In addition, the melting seems to take place in a relative shallow layer at the surface

7   and does not protrude deeply, which would cause the annual layers to mix. The observed variation in

8   EC and dust values could correspond to the findings of Ginot et al. (2014) and Kaspari et al. (2014) that

9   showed annually peaking BC concentrations in the pre-monsoon in Himalayan ice cores. However, for

10   instance, between the ice layers at ca. 65 and 85 cm, no clear peak is observed in EC or dust values

11   (Fig. 12B), which could either indicate that no peak occurred during that particular year, or an ice layer

12   formed at ca. 65 cm in the middle of the year, similarly as potentially at ca. 105 cm.

13   The snow pit covers at best ca. five years of snow accumulation which is certainly a too short time

14   period to make any conclusions on a temporal trend of LAI variations at the site. However, an evident

15   increase in LAI is present, especially in the top 20 cm. Due to the time span of the snow pit we cannot

16   know for certain whether this increase presents a short term pollution event or indicates increasing LAI

17   at the site over a longer time period. We have two hypothesis for the observed increase in EC

18   concentrations and the fraction of dust occurring in the top layer of the snow pit. The higher values may

19   be a consequence of increased ambient EC and dust concentrations in the area, causing increased dry

20   and wet deposition fluxes of these impurities to the glacier, even when assuming constant precipitation.

21   Moreover, as it is f_D that increases, the deposition of dust would have had to increase proportionally

22   more than EC and OC. This could be a result from larger areas in the region being free of snow or

23   changes in the wind characteristics (e.g. stronger winds and/or change in direction). On the other hand,

24   local changes in the net snow mass balance due to a larger fraction of the snow being sublimated in the

25   time period covered by the top 20 cm in comparison to the deeper layers, may partly explain the

26   increased EC and dust absorption values at the top of the pit. Both these basic scenarios can be in effect

27   at the same time.

28   Interestingly, while the EC and OC concentrations and f_D are peaking at the top of the snow pit and

29   potentially decrease very slightly towards the bottom of the snow pit, the absorbing efficiency of EC

30   seems to be decreasing towards the top of the snow pit. We illustrate this in Figure 13 by plotting the

31   ratio between the optical EC from the OCEC-analyzer and the analyzed EC based on TOM, and scale

32   this ratio with the MAC value of 39.8 derived in Figure 3. While the EC concentrations in the snow are

33   the highest at the top of the pit, it appears that at the same time this EC is a less potent light absorber

34   per unit mass (Fig. 13) than in deeper snow layers.
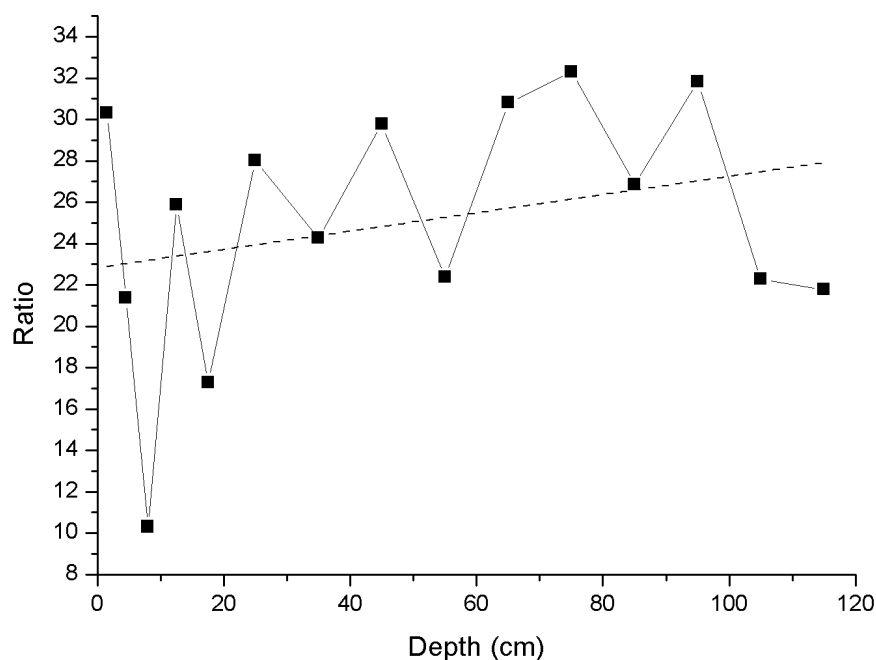
2   Figure 13. The ratio between the optical EC content and analyzed EC content (TOM method) as

3   measured by the OCEC-analyzer using the EUSAAR-2 thermal protocol. The ratio is scaled by the

4   effective MAC value of 39.78 $m^2\,g^{-1}$ derived in Figure 3.

5   **4. Conclusions**

6   Here, first observations of LAI in snow originating from two glaciers in the Indian Himalaya are

7   presented with a method not used widely before to determine LAI in snow. Consisting of a custom built

8   PSAP and an OCEC-analyzer, the attenuation of light is studied on quartz filters, providing estimates

9   on the fraction of light-absorbance caused by non-EC constituents in LAI. Himalayan data display a

10   much greater light-absorbance by dust in the LAI compared to filter samples originating from the

11   seasonal snowpack of Arctic Finland. The role of dust in reducing the snow albedo in this part of

12   Himalayan glaciers needs to be further evaluated, as our results suggest that it might be the dominating

13   LAI in the snow. Our measurements further reveal that the optical properties of EC are different for

14   laboratory generated soot compared to EC originating from snow. With a MAC value off about half of

15   the laboratory EC for the ambient EC particles, it can have potential implications on the snow albedo

16   reduction caused by EC. Over the last approximately five year period in the Himalaya, EC

17   concentrations in the snow are elevated in the top part of the snow pit compared to deeper layers, while

18   at the same time its light absorbing potential is decreasing towards the highest EC-laden layers.

1 Consequently, additional work on the optical properties of EC in snow are needed to enable more

2 accurate estimates of albedo reduction caused by EC in snow, both spatially and temporally.

3 **Acknowledgments**

4 This work has been supported by the Academy of Finland projects: Absorbing Aerosols and Fate of

5 Indian Glaciers (AAFIG; project number 268004) and Greenhouse gas, aerosol and albedo variations

6 in the changing Arctic" (project number 269095). The Academy of Finland Center of Excellence

7 program (project number 272041), as well as the Nordic research and innovation initiative Cryosphere-

8 Atmosphere Interactions in a Changing Arctic Climate have also supported this work. Jonas Svensson

9 is thankful for the support from Svenska kulturfonden. We would like to thank the providers of the soot

10 Consti Taloteknikka, and Göran Lidén at SU luftlab for the mineral samples. The ACES department at

11 Stockholm University, is part of the Bolin centre for climate research. Finally we would like to thank

12 the participants of the AAFIG 2015 expedition, including Sherpas and guides from Real adventure, for

13 their work during the expedition.

14 **References**

15 AMAP: The Impact of Black Carbon on Arctic Climate. Arctic Monitoring and Assessment Programme
16 (AMAP), Oslo, Norway, 72 pp, 2011.
17 Aoki, T., Motoyoshi, H., Kodama, Y., Yasunari, T. J., Sugiura, K., and Kobayashi, H.: Atmospheric
18 aerosol deposition on snow surfaces and its effect on albedo. SOLA, 2, 13–16, doi: 10.2151/sola.2006-
19 004, 2006.
20 Barber, P. W. and Hill, S. C.: Light scattering by particles: Computational methods, World Scientific
21 Publishing, Singapore, 1990.
22 Birch, M. E., and Cary R. A.: Elemental carbon-based method for monitoring occupational exposures,
23 to particulate diesel exhaust, Aerosol. Sci. Technol., 25, 221– 241, 1996.
24 Bolch, T., Kulkarni, A., Kääb, A., Huggel, C., Paul, F., Cogley, J. G., Frey, H., Kargel, J. S., Fujita, K.,
25 Scheel, M., Bajracharya, S., and Stoffel, M.: The State and Fate of Himalayan Glaciers, Science, 336,
26 310–314, doi:10.1126/science.1215828, 2012.
27 Bond, T. C., Anderson, T. L., and Campbell, D.: Calibration and Intercomparison of Filter-Based
28 Measurements of Visible Light Absorption by Aerosols, Aerosol Sci. Technol. 30:582–600, 1999.
29 Bond, T. C., Doherty, S. J., Fahey, D. W., Forster, P. M., Berntsen, T., DeAngelo, B. J., Flanner, M. G,
30 Ghan, S., Kärcher, B., Koch, D., Kinne, S., Kondo, Y., Quinn, P. K., Sarofim, M. F., Schultz, M. G.,
31 Schulz, M., Venkataraman, C., Zhang, H., Zhang, S., Bellouin, N., Guttikunda, S. K., Hopke, P. K.,
32 Jacobson, M. Z., Kaiser, J. W., Klimont, Z., Lohmann, U., Schwarz, J. P., Shindell, D., Storelvmo, T.,
33 Warren, S. G., and Zender, C.S.: Bounding the role of black carbon in the climate system: A scientific
34 assessment, J. Geophys. Res. Atmos., 188, 5380–5552, doi: 10.1002/jgrd.50171, 2013.
35 Bond, T., Bhardwaj, E., Dong, R., Jogani, R., Jung, S., Roden, C., Streets, D. G., and Trautmann, N.:
36 Historical emissions of black and organic carbon aerosol from energy-related combustion, 1850–2000,
37 Global Biogeochem. Cy., 21, doi:10.1029/2006GB002840, 2007.
38 Cachier, H., Bremond, M.P., and Buat-Ménard, P.: Determination of atmospheric soot carbon with a
39 simple thermal method, Tellus Ser.B, 41B, 379-390, 1989.
40 Cavalli, F., Viana, M., Yttri, K.E., Genberg, J., and Putaud, J-P.: Toward a standardised thermal-optical
41 protocol for measuring atmospheric organic and elemental carbon: the EUSAAR protocol, Atmos.
42 Meas. Tech. 3, 79–89, doi:10.5194/amt-3-79-2010, 2010.
43 Chen, L.-W. A., Chow, J. C., Watson, J. G., Moosmüller, H., and Arnott, W. P.: Modeling reflectance
44 and transmittance of quartz-fiber filter samples containing elemental carbon particles: Implications for
45 thermal/optical analysis, J. Aerosol Sci., 35, 765–780, 2004.

Chow, J. C., & Watson, J. G.: PM2:5 carbonate concentrations at regionally representative Interagency monitoring of protected visual environment sites. J. Geophys. Res., 107(D21), 8344, doi:10.1029/2001JD000574, 2002.

Collaud Coen, M., Weingartner, E., Apituley, A., Ceburnis, D., Fierz-Schmidhauser, R., Flentje, H., Henzing, J. S., Jennings, S. G., Moerman, M., Petzold, A., Schmid, O. and Baltensperger, U.: Minimizing light absorption measurement artifacts of the Aethalometer: evaluation of five correction algorithms, Atmos. Meas. Tech., 3, 457–474, 10.5194/amt-3-457-2010, 2010.

Doherty, S. J., Warren, S. G., Grenfell, T. C., Clarke, A. D., and Brandt, R. E.: Light-absorbing impurities in Arctic snow, Atmos. Chem. Phys., 10, 11647–11680, doi: 10.5194/acp-10-11647-2010, 2010.

Doherty, S. J., D. A. Hegg, J. E. Johnson, P. K. Quinn, J. P. Schwarz, C. Dang, and Warren, S.G.: Causes of variability in light absorption by particles in snow at sites in Idaho and Utah, J. Geophys. Res. Atmos., 121, 4751-4768, doi:10.1002/2015JD024375, 2016.

Dumont, M., Brun, E., Picard, G., Michou, M., Libois, Q., Petit, J.-R., Geyer, M., Morin, S., and Josse, B.: Contribution of light-absorbing impurities in snow to Greenland's darkening since 2009, Nat. Geosci., 7, 509–512, doi:10.1038/ngeo2180, 2014.

Forsström, S., Ström, J., Pedersen, C. A., Isaksson, E., and Gerland, S.: Elemental carbon distribution in Svalbard snow, J. Geophys. Res. Atmos., 114, D19112, doi:10.1029/2008JD011480, 2009.

Forsström, S., Isaksson, E., Skeie, R. B., Ström, J., Pedersen, C. A., Hudson, S. R., Berntsen, T. K., Lihavainen, H., Godtliebsen, F., and Gerland, S.: Elemental carbon measurements in European Arctic snow packs, J. Geophys. Res. Atmos., 118, 13614–13627, doi:10.1002/2013JD019886, 2013.

Gautam R., Hsu, N. C., Lau, W. K.-M., and T. J. Yasunari, T. J.: Satellite observations of desert dust-induced Himalayan snow darkening, Geophys. Res. Lett., 40, 988–993, doi:10.1002/grl.50226, 2013.

Gertler, C.G., Puppala, S.P., Panday, A., Stumm, D., Shea, J.: Black carbon and the Himalayan cryosphere: a review. Atmos. Environ. 125, 404–417, doi.org/10.1016/j.atmosenv.2015.08.078, 2016.

Ginot, P., Dumont, M., Lim, S., Patris, N., Taupin, J.-D., Wagnon, P., Gilbert, A., Arnaud, Y., Marinoni, A., Bonasoni, P., and Laj, P.: A 10 year record of black carbon and dust from a Mera Peak ice core (Nepal): variability and potential impact on melting of Himalayan glaciers, The Cryosphere, 8, 1479–1496, doi:10.5194/tc-8-1479-2014, 2014.

Grenfell, T. C., Doherty, S. J., Clarke, A. D., and Warren, S. G.: Spectrophotometric determination of absorptive impurities in snow, Appl. Opt., 50(14), 2037–2048.

Hagler, G. S. W., Bergin, M. H., Smith, E. A., Dibb, J. E., Anderson, C., and Steig, E. J.: Particulate and water-soluble carbon measured in recent snow at Summit, Greenland, Geophys. Res. Lett., 34, L16505, doi:10.1029/2007GL030110, 2007.

Hansen, A.D. A., Kapustin, V. N., Kopeikin, V. M., Gillette, D. A., and Bodhaine, B. A.: Optical absorption by aerosol black carbon and dust in a desert region of central Asia, Atmos. Environ., Part ,4, 27,4, 2527-2531, 1993

Hinds,W. C.: Aerosol Technology,Wiley-interscience, 1999.

Hyvärinen, A.-P., Raatikainen, T., Brus, D., Komppula, M., Panwar, T. S., Hooda, R. K., Sharma, V. P., and Lihavainen, H.: Effect of the summer monsoon on aerosols at two measurement stations in Northern India – Part 1: PM and BC concentrations, Atmos. Chem. Phys., 11, 8271-8282, doi:10.5194/acp-11-8271-2011, 2011.

Immerzeel, W. W., van Beek, L. P. H., and Bierkens, M. F. P.: Climate Change Will Affect the Asian Water Towers, Science, 328, 1382–1385, doi:10.1126/science.1183188, 2010.

Kaspari, S., Painter, T. H., Gysel, M., Skiles, S. M., and Schwikowski, M.: Seasonal and elevational variations of black carbon and dust in snow and ice in the Solu-Khumbu, Nepal and estimated radiative forcings, Atmos. Chem. Phys., 14, 8089–8103, doi:10.5194/acp-14-8089-2014, 2014.

Kääb, A., Berthier, E., Nuth, C., Gardelle, J., and Arnaud, Y.: Contrasting patterns of early 21st century glacier mass change in the Himalaya, Nature, 488, 495–498, doi:10.1038/nature11324, 2012.

Krecl, P., Ström, J., and Johansson, C.: Carbon content of atmospheric aerosols in a residential area during the wood combustion season in Sweden, Atmos. Environ., 41, 6974–6985, 2007.

Lack, D. A. and Cappa, C. D.: Impact of brown and clear carbon on light absorption enhancement, single scatter albedo and absorption wavelength dependence of black carbon, Atmos. Chem. Phys., 10, 4207-4220, doi:10.5194/acp-10-4207-2010, 2010.

Lavanchy, V. M. H., Gäggler, H. W., Schotterer, U., Schwikowski, M., and Baltensperger, U.: Historical record of carbonaceous particle concentrations from a European high-alpine glacier (Colle Gnifetti, Switzerland), J. Geophys. Res., 104, 21227–21236, doi:10.1029/1999JD900408, 1999.

Lim, S., Faïn, X., Zanatta, M., Cozic, J., Jaffrezo, J.-L., Ginot, P., and Laj, P.: Refractory black carbon mass concentrations in snow and ice: method evaluation and inter-comparison with elemental carbon measurement, Atmos. Meas. Tech., 7, 3307-3324, doi:10.5194/amt-7-3307-2014.

Lutz, S., Anesio, A.M., Raiswell, R., Edwards, A., Newton, R.J., Gill, F., and Benning, L.G.: The biogeography of red snow microbiomes and their role in melting arctic glaciers. Nat. Commun. 7: 11968, doi: 10.1038/ncomms11968, 2016.

Meinander, O., Kazadzis, S., Arola, A., Riihelä, A., Räisänen, P., Kivi, R., Kontu, A., Kouznetsov, R., Sofiev, M., Svensson, J., Suokanerva, H., Aaltonen, V., Manninen, T., Roujean, J.-L., and Hautecoeur, O.: Spectral albedo of seasonal snow during intensive melt period at Sodankylä, beyond the Arctic Circle, Atmos. Chem. Phys., 13, 3793-3810, doi:10.5194/acp-13-3793-2013, 2013.

McConnell, J. R., Edwards, R., Kok, G. L., Flanner, M. G., Zender, C. S., Saltzman, E. S., Banta, J. R., Pasteris, D. R., Carter, M. M., and Kahl, J. D. W.: 20th century industrial black carbon emissions altered arctic climate forcing, Science, 317, 1381–1384, doi:10.1126/science.1144856, 2007.

Ming, J., Cachier, H., Xiao, C., Qin, D., Kang, S., Hou, S., and Xu, J.: Black carbon record based on a shallow Himalayan ice core and its climatic implications, Atmos. Chem. Phys., 8, 1343– 1352, doi:10.5194/acp-8-1343-2008, 2008.

Ming, J., Xiao, C., Du, Z., and Yang, X.: An Overview of Black Carbon Deposition in High Asia Glaciers and its Impacts on Radiation Balance, Adv.Water Resour., 55, 80–87, 2013.

Ming, J., Wang, Y., Du, Z., Zhang, T., Guo, W., Xiao, C., Xu, X., Ding, M., Zhang, D., and Yang, W.: Widespread albedo decreasing and induced melting of Himalayan snow and ice in the early 21st century. PLoS One 10(6):e0126235. doi:10.1371/journal.pone.0126235, 2015.

Painter, T. H., Barrett, A. P., Landry, C. C., Neff, J. C., Cassidy, M. P., Lawrence, C. R., McBride, K. E., and Farmer, G. L.: Impact of disturbed desert soils on duration of mountain snow cover, Geophys. Res. Lett., 34, L12502, doi:10.1029/2007GL030284, 2007.

Painter, T. H., Skiles, S. M., Deems, J. S., Bryant, A. C., and Landry C.C.: Dust radiative forcing in snow of the Upper Colorado River Basin: 1. A 6 year record of energy balance, radiation, and dust concentrations. Water Resources Research, 48, doi: 10.1029/2012wr011985, 2012.

Qian,Y., Yasunari, T. J., Doherty, S. J., Flanner, M. G., Lau, W. K., Ming, J., Zhang, R.: Light-absorbing particles in snow and ice: measurement and modeling of climatic and hydrological impact. Adv. Atmos. Sci. 32(1),64–91, doi: 10.1007/s00376-014-0010-0, 2015.

Qu, B., Ming, J., Kang, S.-C., Zhang, G.-S., Li, Y.-W., Li, C.-D., Zhao, S.-Y., Ji, Z.-M., and Cao, J.-J.: The decreasing albedo of the Zhadang glacier on western Nyainqentanglha and the role of light-absorbing impurities, Atmos. Chem. Phys., 14, 11117-11128, doi:10.5194/acp-14-11117-2014, 2014.

Ruppel, M. M., Isaksson, E., Ström, J., Beaudon, E., Svensson, J., Pedersen, C. A., and Korhola, A.: Increase in elemental carbon values between 1970 and 2004 observed in a 300-year ice core from Holtedahlfonna (Svalbard), Atmos. Chem. Phys., 14, 11447-11469, doi:10.5194/acp-14-11447-2014, 2014.

Raatikainen, T., Brus, D., Hooda, R. K., Hyvärinen, A.-P., Asmi, E., Sharma, V. P., Arola, A., and Lihavainen, H.: Size-selected black carbon mass distributions and mixing state in polluted and clean environments of northern India, Atmos. Chem. Phys., 17, 371-383, doi:10.5194/acp-17-371-2017, 2017.

Schmitt, C. G., All, J. D., Schwarz, J. P., Arnott, W. P., Cole, R. J., Lapham, E., and Celestian, A.: Measurements of light-absorbing particles on the glaciers in the Cordillera Blanca, Peru, The Cryosphere, 9, 331-340, doi:10.5194/tc-9-331-2015, 2015.

Schwarz, J. P., Doherty, S. J., Li, F., Ruggiero, S. T., Tanner, C. E., Perring, A. E., Gao, R. S., and Fahey, D. W.: Assessing Single Particle Soot Photometer and Integrating Sphere/Integrating Sandwich Spectrophotometer measurement techniques for quantifying black carbon concentration in snow, Atmos. Meas. Tech., 5, 2581–2592, doi:10.5194/amt-5-2581-2012, 2012.

Schwarz, J. P., Gao, R. S., Perring, A. E., Spackman, J. R., and Fahey, D.W.: Black carbon aerosol size in snow, Nat. Sci. Reports, 3, 1356, doi:10.1038/srep01356, 2013.

Shindell, D., Kuylenstierna, J. C. I., Vignati, E., van Dingenen, R., Amann, M., Klimont, Z., Anenberg, S. C., Muller, N., JanssensMaenhout, G., Raes, F., Schwartz, J., Faluvegi, G., Pozzoli, L., Kupiainen,

K., Höglund-Isaksson, L., Emberson, L., Streets, D., Ramanathan, V., Hicks, K., Oanh, N. T. K., Milly, G., Williams, M., Demkine, V., and Fowler, D.: Simultaneously Mitigating Near-Term Climate Change and Improving Human Health and Food Security, Science, 335, 183–189, doi: 10.1126/science.1210026, 2012.

Svensson, J. Ström, J., Hansson, M., Lihavainen, H., and Kerminen, V.-M.: Observed metre scale horizontal variability of elemental carbon in surface snow, Environ. Res. Lett., 8, 034012, doi:10.1088/1748-9326/8/3/034012, 2013.

Svensson J., Virkkula A., Meinander O., Kivekäs N., Hannula H.-R., Järvinen O., Peltoniemi J.I., Gritsevich M., Heikkilä A., Kontu A., Neitola K., Brus D., Dagsson-Waldhauserova P., Anttila K., Vehkamäki M., Hienola A., de Leeuw G. & Lihavainen H. 2016: Soot-doped natural snow and its albedo — results from field experiments. Boreal Env. Res. 21: 481–503.

Thevenon, F., Anselmetti, F. S., Bernasconi, S. M., and Schwikowski, M.: Mineral dust and elemental black carbon records from an Alpine ice core (Colle Gnifetti glacier) over the last millennium, J. Geophys. Res., 114, 102, doi: 10.1029/2008JD011490, 2009.

Virkkula, A., Ahlquist, N. C., Covert, D. S., Arnott,W. P., Sheridan, P. J., Quinn, P. K., and Coffman, D. J. (2005). Modification, Calibration and a Field Test of an Instrument for Measuring Light Absorption by Particles, Aerosol Sci. Technol. 39:68–83.

Warren, S. G., and Wiscombe, W. J.: A model for the spectral albedo of snow. II: Snow containing atmospheric aerosols, J. Atmos. Sci., 37, 2734–2745, 1980.

Wang, M., Xu, B., Zhao, H., Cao, J., Joswiak, D., Wu, G., and Lin, S.: The Influence of Dust on Quantitative Measurements of Black Carbon in Ice and Snow when Using a Thermal Optical Method, Aerosol Sci. Technol., 46, 60–69, doi:10.1080/02786826.2011.605815, 2012.

Xu, B., Yao, T., Liu, X., and Wang, N.: Elemental and organic carbon measurements with a two-step heating-gas chromatography system in snow samples from the Tibetan Plateau, Ann. Glaciol., 43, 257–262, 2006.

Xu, B., Cao, J., Hansen, J., Yao, T., Joswiak, D.R., Wang, N., Wu, G., Wang, M., Zhao, H., Yang, W., Liu, X., and He, J.: Black soot and the survival of Tibetan glaciers. Proc. Nat. Acad. Sci. USA, 106, 22114–22118, doi:10.1073/pnas.0910444106, 2009.

Yang, S., Xu, B., Cao, J., Zender, C. S., and Wang, M.: Climate effect of black carbon aerosol in a Tibetan Plateau glacier, Atmos. Environ., 111, 71–78, doi.org/10.1016/j.atmosenv.2015.03.016 1352-2310, 2015.

1 Table 1. Snow pit filter samples from Sunderdhunga 2015. Durga kot glacier snow pits are A-D and Bhanolti glacier snow pit E.

Snow pit ID and elevation (m a.s.l.)	Sample interval (cm)	τTOT	τD	τEC	EC TOM (g m⁻²)	EC optical (g m⁻²)	eEC (g m⁻²)	Total C (g m⁻²)	EC (µg L⁻¹)	F$_D$
A, 4869	0-2	3.94	2.63	1.31	0.09	0.05	0.03	1.75	362.18	66.68
	2-5	-	-	-	0.25	0.00	-	0.25	1010.62	-
	5-10	-	-	-	0.30	0.01	-	11.11	1030.84	-
B, 4921	0-2	0.69	0.26	0.43	0.01	0.01	0.01	0.15	40.33	37.64
	2-6	-	4.79	-	0.13	0.04	-	4.24	398.60	-
C, 4921	0-3	0.29	0.16	0.13	0.01	0.00	0.00	0.21	35.71	56.62
	3-6	1.76	1.32	0.44	0.03	0.02	0.01	1.24	55.15	75.12
	6-9	-	5.19	-	0.15	0.00	-	4.88	1095.79	-
	9-13	2.20	1.35	0.84	0.06	0.03	0.02	0.76	381.63	61.57
D, 4950	0-5	0.11	0.07	0.04	0.00	0.00	0.00	0.06	13.20	66.65
	5-10	-	-	-	0.07	0.01	-	6.70	327.14	-
	10-20	1.37	0.94	0.43	0.04	0.02	0.01	0.64	220.21	68.63
	20-30	1.15	0.66	0.49	0.02	0.02	0.01	0.34	78.58	57.36
E, 5008	0-3	1.81	1.41	0.40	0.02	0.02	0.01	1.27	65.73	77.87
	3-6	3.25	1.97	1.27	0.08	0.04	0.03	1.45	272.57	60.77
	6-10	5.88	4.09	1.79	0.12	0.03	0.05	3.58	607.83	69.55
	10-15	2.94	1.77	1.17	0.06	0.04	0.03	0.97	233.21	60.32
	15-20	0.98	0.32	0.66	0.04	0.02	0.02	0.30	111.42	33.05
	20-30	1.06	0.52	0.54	0.02	0.02	0.01	0.23	140.71	49.15
	30-40	1.04	0.41	0.63	0.03	0.02	0.02	0.21	105.55	39.61
	40-50	1.03	0.38	0.65	0.02	0.02	0.02	0.21	98.15	36.71
	50-60	2.10	1.04	1.06	0.06	0.04	0.03	0.66	269.67	49.53
	60-70	2.75	1.10	1.65	0.07	0.06	0.04	0.49	179.30	39.90
	70-80	1.21	0.44	0.77	0.02	0.02	0.02	0.19	93.00	36.12
	80-90	0.91	0.33	0.59	0.02	0.02	0.01	0.15	72.80	35.81

90-100	1.65	0.73	0.92	0.04	0.03	0.02	0.31	143.80	43.95
100-110	0.57	0.17	0.40	0.02	0.01	0.01	0.15	79.31	29.54
110-120	0.46	0.12	0.34	0.02	0.01	0.01	0.15	56.91	25.68